On Velocity Estimation Using Speckle Decorrelation

Pai-Chi Li, *Member, IEEE*, Chong-Jing Cheng, and Chih-Kuang Yeh

***Abstract*—Quantitative estimation of blood velocity using Doppler techniques is fundamentally limited because only the axial component can be detected. Speckle decorrelation resulting from scatterer motion may be used to compute non-axial components and to obtain quantitative flow information. Based on both simulations and experimental results, it is shown that the decorrelation technique is feasible only for constant flows. If flow gradients are present, the correlation between two signals along the same line of observation may be significantly affected by the gradients. Therefore, the decorrelation method cannot be used for quantitative flow estimation if flow gradients are not accurately measured and effects on signal correlation are not fully compensated. Results in this paper show that accurate estimation of flow gradients is practically difficult. It is further shown that effects of signal-to-noise ratio (SNR) on the correlation must also be taken into account for quantitative flow analysis.**

I. Introduction

Quantitative estimation of blood velocity using conventional Doppler techniques has not been successful because only the axial component of the velocity vector can be estimated. Projection of the velocity vector onto transverse directions does not produce Doppler shifts. Therefore, non-axial flows are not detectable using Doppler techniques. To obtain transverse and elevational velocity components, several correlation-based methods were presented [1]–[4]. The correlation methods are based on the fact that when a group of randomly distributed scatterers moves across an acoustic beam, the received signals decorrelate as a function of time. Therefore, blood velocity can be estimated by measuring the correlation function. The speckle decorrelation-based velocity estimation technique using RF ultrasound signals will also be referred to as the correlation method throughout this paper.

In [1], it was shown that using the spatial and temporal correlation function of the RF signals, both axial and lateral motion can be estimated. Based on a similar model, it was also shown that the velocity vector can be obtained by using only a few correlation coefficients [2]. The correlation method was also applied to intravascular ultrasound (IVUS) [3]–[4]. In IVUS, the blood direction is orthogonal to the imaging plane. By measuring the rate of speckle decorrelation, blood speed information can be obtained. A finite-impulse response (FIR) filter bank suitable for real-time blood speed imaging was also proposed to estimate the decorrelation rate [4].

An inherent assumption of these correlation methods is that blood velocity is constant within the sample volume. In many clinical applications, however, flow gradients are present. Because flow gradients also result in signal decorrelation, effects of flow gradients must be considered for accurate velocity estimation using speckle decorrelation [5]. It is the primary purpose of this paper to study effects of flow gradients on speckle decorrelation. Influence of SNR on the correlation will also be addressed.

This paper is organized as follows. Section II describes basic principles of the correlation-based method. Both simulations and experimental results of constant scatterer motion will be presented. Effects of flow gradients will be simulated in Section III and experimentally studied in Section IV. An analysis on effects of SNR will also be included in Section IV. The paper concludes in Section V.

II. Basic Principles of the Correlation Method

A. Theory

Effects of lateral motion on signal correlation are illustrated in Fig. 1. The upper panel shows that a group of scatterers moves laterally across the sample volume. Backscattered signals acquired before (solid) and after (dotted) the movement are shown in the lower panel. For fully developed speckle (i.e., homogeneous distribution of scatterers with a uniform scattering strength and uncorrelated microscopic structures), the correlation as a function of scatterer displacement can be derived [6].

Assuming a linear imaging system with a space invariant point spread function, a received echo can be represented as the convolution of the system's point spread function and the scatterer distribution function. Let $a(\bullet)$ be the scatterer distribution function and $b(\bullet)$ be the system's point spread function, the received signal $s(\bullet)$ is

$$s(u) = \int_{-\infty}^{\infty} a(u')b(u-u')du' \qquad (1)$$

where analytic signal representation is used with a three-dimensional coordinate system denoted by $u = (x, y, z)$.

Manuscript received August 29, 2000; accepted January 30, 2001. Support from National Scier-ce Council under grant NSC-89-2213-E-002-041 is gratefully appreciated.

The authors are with the Department of Electrical Engineering, National Taiwan University, Taipei, Taiwan, R.O.C (e-mail: paichi@cc.ee.ntu.edu.tw).

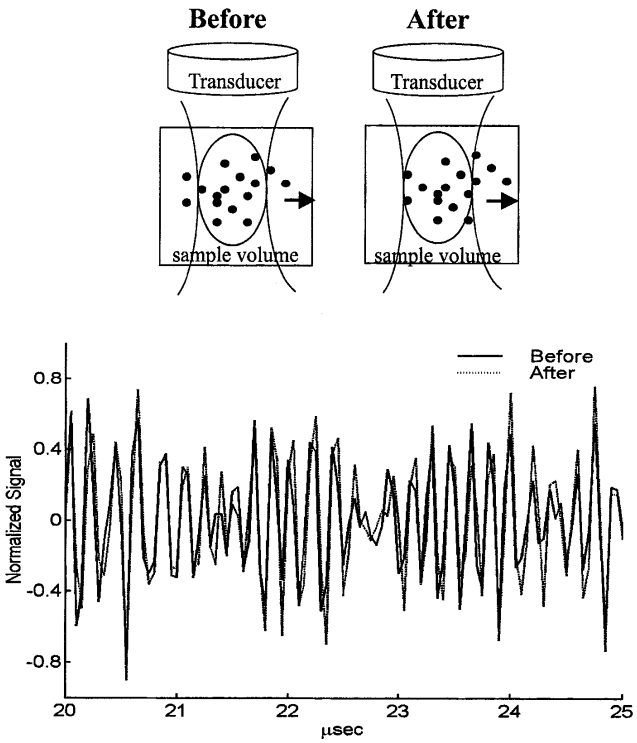

Fig. 1. Effects of lateral movement on the received signal. The solid line is before movement, and the dotted line is after movement.

The complex cross-correlation function $c(u_1, u_2)$ of two received echoes, $s_1(u_1)$ and $s_2(u_2)$, is

$$c(u_1,u_2)\equiv<s_1(u_1)s_2^*(u_2)>=\iint_{-\infty}^{\infty}<a(u')a^*(u''-u_0)>b(u_1-u')b^*(u_2-u'')du'du'' \quad (2)$$

where $<*>$ represents the ensemble average and u_0 is the scatterer displacement between the two measurements. Because the insonified region is fully developed speckle, we have

$$<a(u')a^*(u''-u_0)>=a_0^2\delta(u'-u''+u_0) \quad (3)$$

where $\delta(*)$ is the three-dimensional Dirac-delta function and a_0 is the scattering strength. Hence, (2) can be rewritten as

$$c(u_1,u_2)=a_0^2\int_{-\infty}^{\infty}b(u_1-u')b^*(u_2-u'-u_0)du'. \quad (4)$$

The cross-correlation function is typically evaluated at $u_1 = u_2$. In this case, (4) becomes

$$\begin{aligned}c(u_1,u_1)&=a_0^2\int_{-\infty}^{\infty}b(u_1-u')b(u_1-u'-u_0)du'\\&=a_0^2\int_{-\infty}^{\infty}b(u''')b(u'''-u_0)du'''.\end{aligned} \quad (5)$$

Eq. (5) shows that correlation between two signals from the same sample volume can be represented by the autocorrelation function of the system's point spread function [6].

If the movement is only in the lateral direction, (5) can be applied to estimate lateral velocity, assuming that the lateral radiation pattern is known. If axial movement is also present, the axial velocity can be found by finding the peak of the cross-correlation function. As shown in Fig. 2(a), the solid line represents a signal, and the dotted line represents the signal with axial movement after a pulse repetition interval (PRI). The normalized cross-correlation function of the two signals is shown in Fig. 2(b). Peak of the correlation function is temporally shifted from zero because of the axial movement, but its value remains close to unity. In other words, it is assumed that the original scatterers remain in the image plane after motion. Fig. 2(c and d) shows the received signals and the corresponding cross-correlation function with only lateral motion. As shown in Fig. 2(d), lateral motion changes scatterer distribution, thus reducing the peak value of the normalized cross-correlation function from one. Nevertheless, the peak position is not shifted because there is no axial motion. As described in (1)–(5), the decorrelation (i.e., decrease in correlation coefficient) is directly related to the lateral radiation pattern. Thus, the lateral velocity can be obtained if the lateral radiation pattern is known. Fig. 2(e and f) shows the received signals and the corresponding cross-correlation function with both lateral and axial motion. In this case, the cross-correlation function is temporally shifted, and its peak value becomes smaller than one. Again, both lateral and axial velocities can be found by using the correlation function.

B. Experiments

Experiments were performed to test these principles. The data acquisition system consisted of a pulser/receiver (Panametrics 5072PR, MA), an arbitrary function generator (Hewlett-Packard E1445A, CA), and a 12-bit, 20-Msamples/s A/D (Hewlett-Packard E1429A, CA). Hewlett-Packard Interface Bus (HPIB) was used for communication between the data acquisition unit and a personal computer. The transducer (Panametrics V308, MA) was positioned by a three-dimensional step motor system (Q-sync; Hsin-Chu, Taiwan, R.O.C.). The circular transducer had a focus at 7 cm, a 5-MHz center frequency, and a 1.9-cm diameter. A gelatin phantom with uniformly distributed glass beads (Sigma G4649, St. Louis, MO) was constructed to generate speckle signals. Diameter of the glass beads was smaller than 106 μm. Glass beads were added with a concentration close to its saturation level.

In the first experiment, the transducer was moved laterally with a step of 20 μm. At each step, RF data were acquired before being demodulated to baseband. Using the complex baseband data, correlation coefficients were calculated using the data within a 1-μs window at a depth of 6.7 cm (i.e., 90-μs round-trip time of flight). The 1-μs window length was chosen such that both adequate SNR and sufficient axial resolution could be achieved. The correlation coefficient in this case is defined as the zeroth lag value of the normalized cross-correlation function.

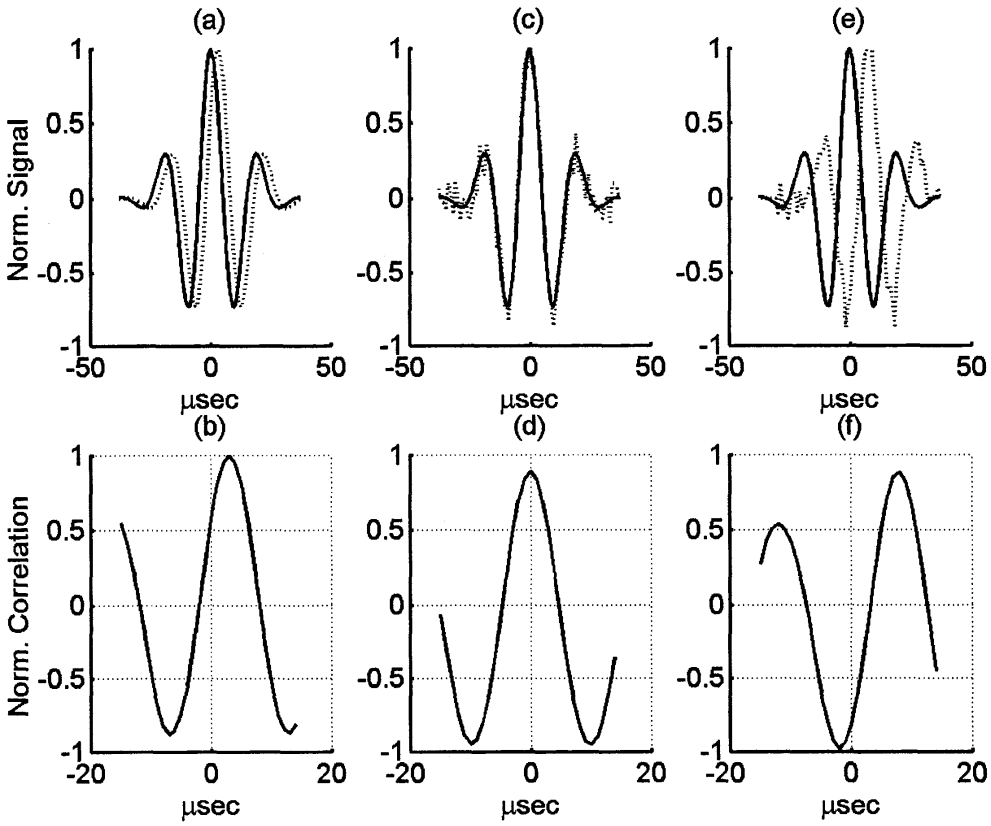

Fig. 2. Effects of lateral and axial movement on the correlation function. Panel a shows the normalized signal before (solid) and after (dotted) axial movement. The normalized cross-correlation function is shown in panel b. Panels c and d and panels e and f have the same format as panels a and b. Panels c and d are for lateral movement only, and panels e and f are for both lateral and axial movement.

Fifty correlation coefficients of the same lateral displacement were averaged to get a mean value. The results are shown as the dashed line in Fig. 3. The solid line in Fig. 3 shows the normalized radiation pattern measured by the same setup, except that the speckle phantom was replaced with a nylon wire located at the same depth. The dashed line shows the correlation coefficients with error bars indicating ± 1 standard deviation. As predicted by (5), the two curves had good agreement. Therefore, lateral velocity can be found given a correlation coefficient and the lateral radiation pattern.

As previously mentioned, the correlation-based method can also be extended to measure flows with both lateral and axial motion. To emulate such flows using the gelatin phantom, the transducer was moved 20 μm laterally and 25 μm axially per data acquisition step. The dot-dashed line in Fig. 4 shows correlation coefficients at a depth of 8.1 cm (i.e., 110-μs round-trip time of flight) using the zero-th lag of the normalized cross-correlation function. As a reference, data were also acquired from the same depth region by moving the transducer only in the lateral direction. The correlation coefficients with only lateral movement are shown as the dotted line. Using the zero-th lag, axial motion is not compensated, and correlation coefficients decrease faster than the reference curve (i.e., the dotted line). The axial motion can be compensated by using the peak value of the normalized cross-correlation function instead of the zero-th lag value. With axial motion compensation, the correlation coefficients shown as the solid line in Fig. 4 closely match the reference curve. In other words, both axial and lateral motion can be estimated using the correlation method. The error bars associated with the solid line in Fig. 4 represent ± 1 standard deviation. As in Fig. 3, it is shown that the standard deviation increases as the mean correlation coefficient decreases.

III. Flows with Velocity Gradients: Simulations

The experiments in Section II had constant motion within the sample volume. For blood flow measurements, however, flow gradients are present and cannot be ignored. Flow gradients cause relative scatterer motion within the sample volume and result in additional signal decorrelation. Thus, such effects must be compensated when correlation is used for velocity estimation.

Laminar flows were considered in this paper. The simulation model developed by A. T. Kerr and J. W. Hunt was adopted [7]. The model takes into account both amplitude and temporal responses given the transducer geometry. The acoustic response of a scatterer is calculated us-

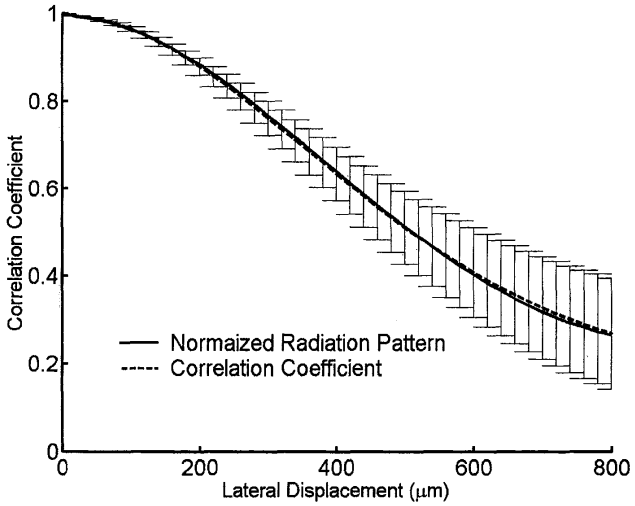

Fig. 3. Correlation coefficient as a function of lateral displacement (dashed) vs. normalized radiation pattern (solid). Error bars represent ±1 standard deviation of the estimated correlation coefficients.

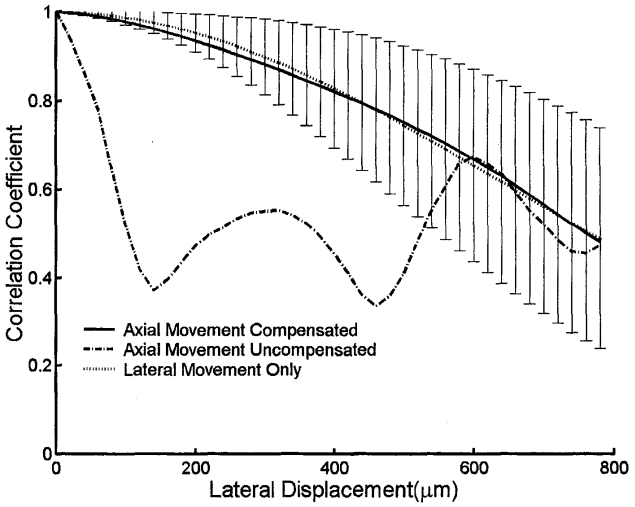

Fig. 4. Correlation coefficient with (solid) and without (dot-dashed) axial movement compensation. The dotted line is the reference curve with only lateral movement. Error bars represent ±1 standard deviation.

ing the acoustic impulse response method. In other words, output of the transducer $V(t)$ can be expressed by

$$V(t) = \xi \cdot P_e(t) * h_r(\vec{r}, t) * h_t(\vec{r}, t) \tag{6}$$

where ξ is a constant and $*$ is the convolution operator. The pulse-echo response $P_e(t)$ is assumed Gaussian, and $h_r(\vec{r}, t)$ and $h_t(\vec{r}, t)$ are receive and transmit acoustic impulse responses, respectively. The model assumes point scatterers randomly distributed on a two-dimensional grid.

In the simulations, the transducer had a center frequency of 5 MHz and a 1.9-cm aperture size. The sample volume was located at focus, which was 7 cm away from the transducer face. The sound velocity was 1540 m/s, and

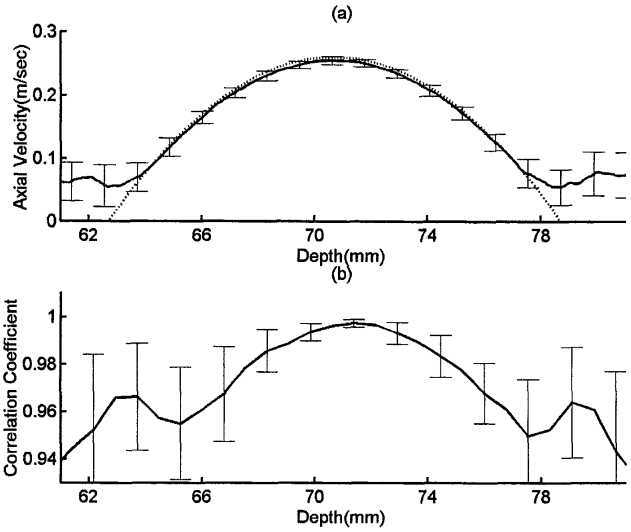

Fig. 5. Axial velocity (a) and correlation coefficient (b) as a function of depth. The error bars denote ±1 standard deviation.

the PRI was 100 μs. The laminar flow had a parabolic velocity profile shown as the following

$$v(r) = V_{MAX} \cdot \left[1 - \left(\frac{r}{R}\right)^2\right] \tag{7}$$

where R is radius of the vessel, V_{MAX} is the maximum flow velocity, and r is radial distance from the center of vessel. The maximum velocity and the Doppler angle in the simulations were 30 cm/s and 30°, respectively. The projected peak velocity along the axial direction is 26 cm/s. The radius of the vessel was 4 mm in the simulations.

The estimated axial velocity is shown as the solid line in Fig. 5(a). The horizontal axis represents the depth from the transducer. Axial velocity was calculated using the auto-correlation approach described in [8]. In other words, velocity was calculated based on the phase of the first lag of the auto-correlation of the slow-time flow signal. Note that the auto-correlation approach uses the slow-time signal, whereas the decorrelation method uses the fast-time signal. The estimated velocity had good agreement with the actual velocity shown as the dotted line in Fig. 5(a). Fig. 5(b) shows correlation coefficients under the same conditions. The correlation coefficients were calculated using the peak value of the cross-correlation function of two signals separated by one PRI. One hundred data sets with different initial scatterer distribution were generated. The solid lines in Fig. 5(a and b) demonstrate the mean values, and the error bars span ±1 standard deviation using the 100 data sets.

It is shown in Fig. 5(a) that axial velocity estimation is robust even in the presence of velocity gradients. The correlation coefficients shown in Fig. 5(b), on the other hand, are significantly affected by flow gradients. In Section II, it was shown that the correlation coefficient decreases as the velocity of a constant flow increases. Because the velocity of a laminar flow is zero at the vessel wall and reaches a

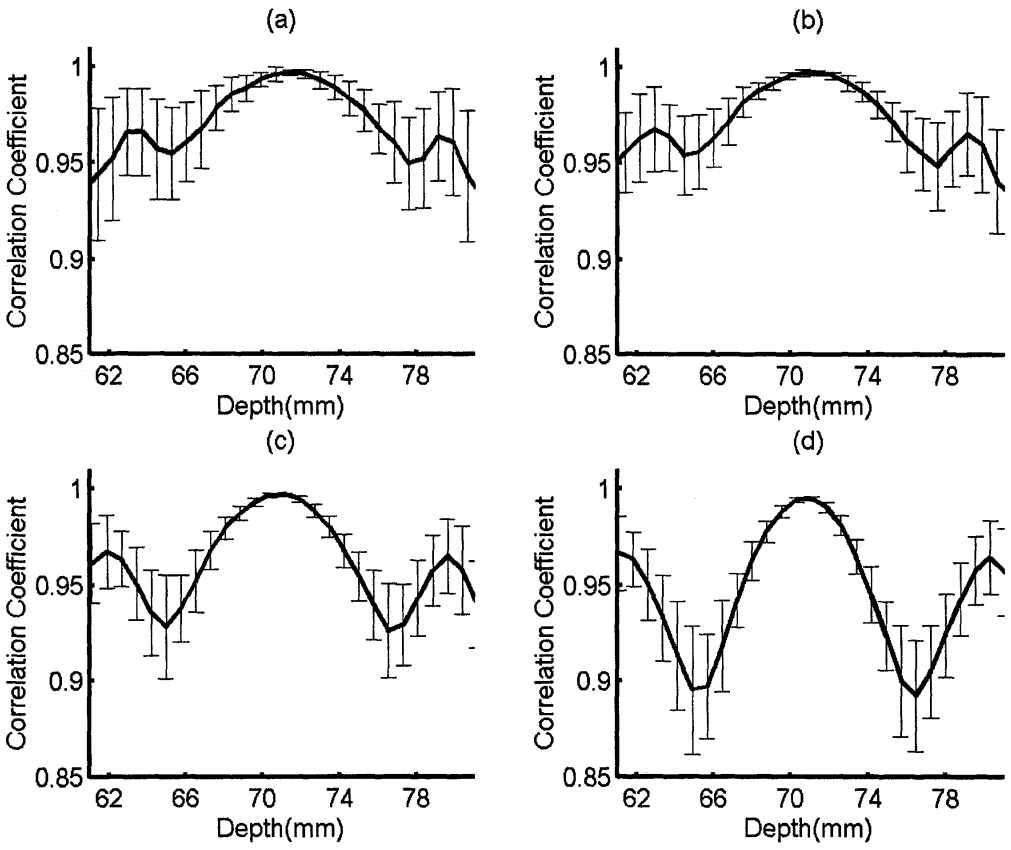

Fig. 6. Four correlation kernel sizes: a) 1 μs, b) 2 μs, c) 4 μs, and d) 6 μs.

maximum at the center, a high correlation coefficient near the wall and a low correlation coefficient at the center may be expected. Because of flow gradients, however, Fig. 5(b) shows that the correlation coefficient is the largest at the center and starts to decreases as it moves away from the center. This is consistent with the fact that the flow gradient, defined as the spatial derivative of velocity, is the largest at the vessel wall and the smallest at the center. Thus, it is difficult to estimate the flow velocity using the correlation coefficient if effects of flow gradients are not compensated.

Several problems may be encountered when estimating the gradients. First, because a gradient is the spatial derivative of velocity, errors in the velocity estimation become more pronounced in the gradient. As shown by the error bars in Fig. 5(a), non-negligible velocity estimation errors exist using the relatively robust auto-correlation approach. Such errors in turn affect accuracy of the velocity estimation. The second problem is the errors of correlation coefficient calculations. As shown by the error bars in Fig. 5(b), the standard deviation, in most cases, is comparable with the difference from unity. Thus, a small error in correlation coefficient may lead to a significant error in the estimated velocity. Although averaging can be applied to reduce such errors, utility of the correlation method in real-time applications is severely limited with averaging.

With flow gradients, speckle decorrelation is also affected by sample volume size. For a given flow gradient, the correlation coefficient decreases as the size of the sample volume increases. Therefore, a possible method to minimize effects of the flow gradient is to utilize the change in speckle correlation with different sample volume sizes. Fig. 6 shows the change of speckle decorrelation as a function of correlation kernel size. Panels a, b, c, and d correspond to a correlation kernel size of 1, 2, 4, and 6 μs, respectively. The decrease in correlation coefficient with increased kernel size is clearly visible. Generally, the correlation coefficient in the region of large gradients (e.g., near the vessel walls) decreases more rapidly as the correlation length increases. In all cases, the standard deviation limits the potential utility of the correlation method unless signal averaging is applied.

IV. Flows with Velocity Gradients: Experiments

Experiments were also conducted to study correlation in the presence of flow gradients. The experimental setup is shown in Fig. 7. The transducer and the data acquisition system were the same as the ones used in previous experiments. A blood-mimicking fluid (Shelley Medical Imaging Technologies, Ontario, Canada) was used instead of the gelatin phantom. The fluid was driven by a peristal-

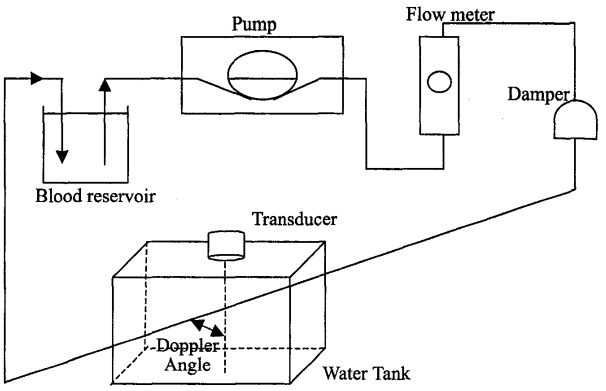

Fig. 7. Experimental setup for data acquisition with a blood-mimicking fluid.

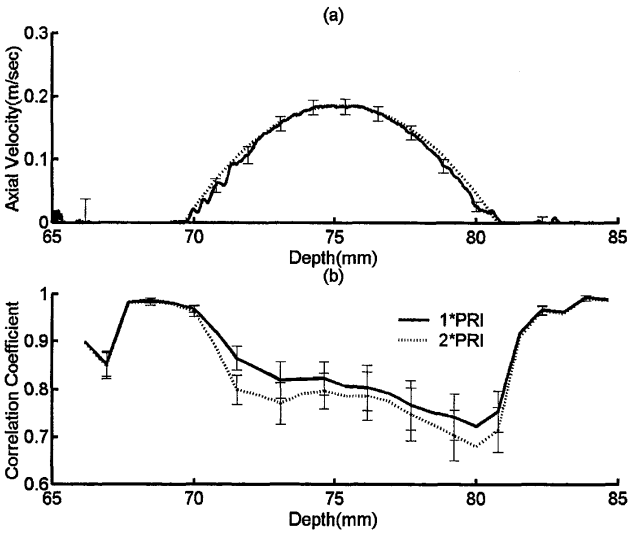

Fig. 8. Axial velocity (a) and correlation coefficient (b) as a function of depth. The error bars denote ±1 standard deviation. The solid line in panel b represents correlation coefficient with one PRI interval, and the dotted line is with two PRI interval.

sis pump (Model 77201-60, Cole-Parmer, IL) in a silicone peroxide-cured tube (L/S-18, Cole-Parmer, IL). A damper (625 E, Cole-Parmer, IL) was used to eliminate pulsation in the output flow. A flow meter was use to monitor the volume flow rate for comparisons with the measurements. The tube was located at the focal region of the transducer. Flow signals were sampled at a PRI of 200 μs. The Doppler angle was 54°. As in the simulations, a total of 100 data sets were collected, and results were averaged to obtain the mean and the standard deviation.

The solid line in Fig. 8(a) shows the mean axial velocity obtained from the auto-correlation method with the error bars indicating ±1 standard deviation. The dotted line shows an ideal parabolic laminar profile with the maximum velocity equal to 32 cm/s (18.8 cm/s after projection on the axial direction). The vessel diameter was 0.95 cm. The corresponding correlation coefficients were shown in Fig. 8(b). The solid line and the dotted line represent the correlation coefficients obtained from cross-correlating two signals separated by one PRI (i.e., 200 μs) and two PRIs (i.e., 400 μs), respectively. Note that although the estimated axial velocity fits well to an ideal laminar profile, the correlation coefficients are substantially different from the simulation results shown in Fig. 5(b). The four panels of Fig. 9 illustrate effects of the correlation kernel size on correlation coefficient. Again, the four kernel sizes correspond to 1, 2, 4, and 6 μs. Similar to Fig. 6, the sample volume size clearly affects the estimated correlation coefficient. However, the general trend is different from that of Fig. 6. The mean correlation coefficient may increase with a larger correlation kernel.

The differences between simulations and experiments are mainly due to the finite SNR of the experimental data. Simulations were performed to demonstrate effects of the SNR on signal correlation. Simulation parameters were identical to those used in Fig. 5. Fig. 10 and Fig. 11 show correlation coefficients for two signals separated by one PRI interval (solid line) and two PRIs (dotted line). Noise was not considered in Fig. 10. In Fig. 11, on the other hand, noise was included before the calculation, and the SNR was equal to 9.5 dB. The SNR is defined as the ratio of the average signal power to the average noise power. Fig. 10 shows that without noise, the decrease in correlation coefficient from unity roughly doubles as the time interval between the two signals doubles in this region. In other words, the correlation coefficient is approximately linear as a function of the lateral movement in this case. With the addition of noise, Fig. 11 demonstrates an overall decrease in the correlation coefficient. Such effects were also described in [5].

The SNR in Fig. 11 is constant over the entire depth. In practice, the SNR may change with depth depending on attenuation and the system's time gain compensation. The SNR of the previous experimental data was plotted in Fig. 12 as a function of depth. Range of the vessel was approximately from 70 to 80 mm. Because of acoustic attenuation of the blood-mimicking fluid and the constant receiver gain, it is shown that the SNR decreases with depth. This is consistent with the fact that the correlation coefficient shown in Fig. 8(b) also decreased with depth. Note that, to calculate the SNR of the experimental data, the signal power was obtained by calculating the average signal intensity over 100 repetitive measurements. On the other hand, the noise power was measured at the vessel walls. Because the vessel was stationary, average intensity of the signals from vessel over 100 measurements was used as a reference. Then, the difference between each individual measurement and the reference signal was viewed as noise in calculating the SNR.

V. Concluding Remarks

In this paper, flow velocity estimation using speckle decorrelation was discussed. It was shown that flow velocity can be estimated using the correlation method only if effects of flow gradients and SNR on the correlation can

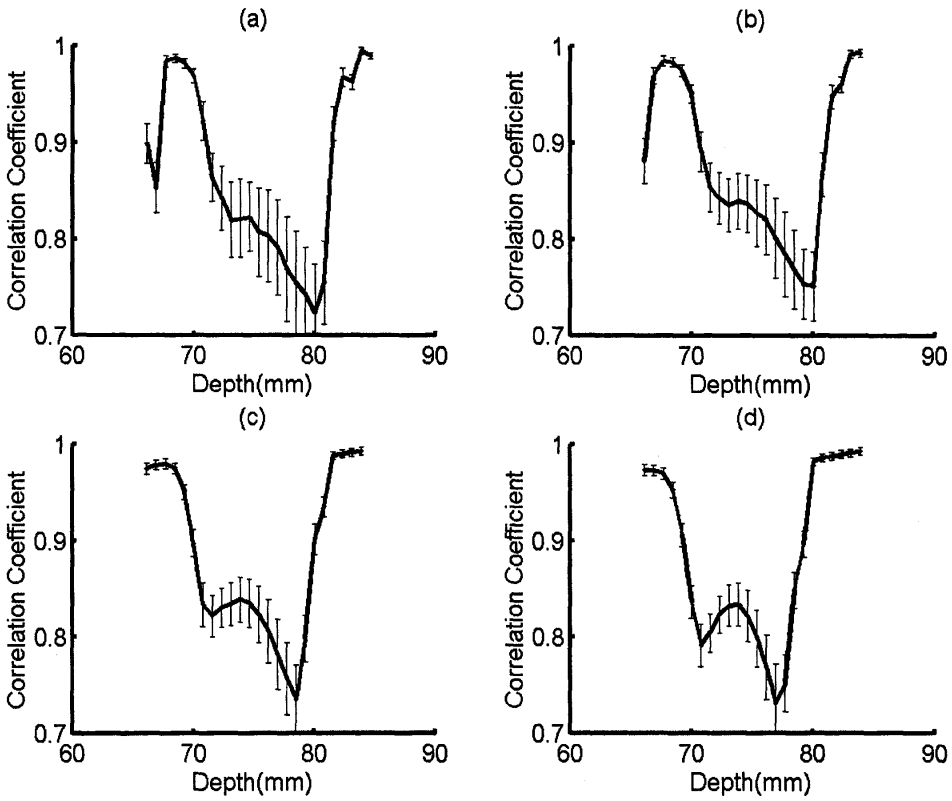

Fig. 9. Four correlation kernel sizes: a) 1 μs, b) 2 μs, c) 4 μs, and d) 6 μs.

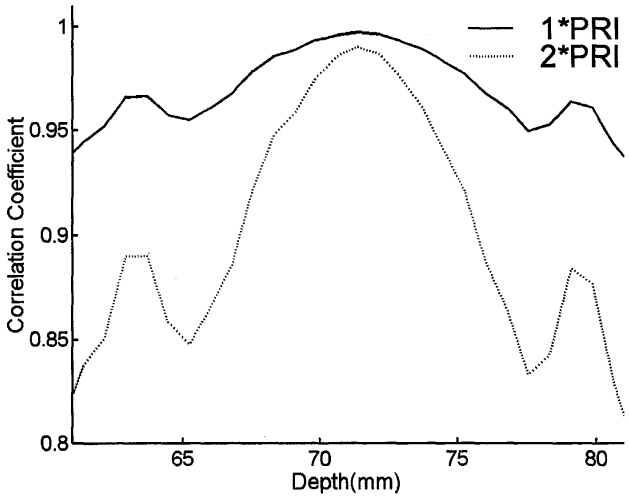

Fig. 10. Correlation coefficient as a function of depth with no added noise. Solid is for two signals separated by one PRI, and dotted is for two signals separated by two PRIs.

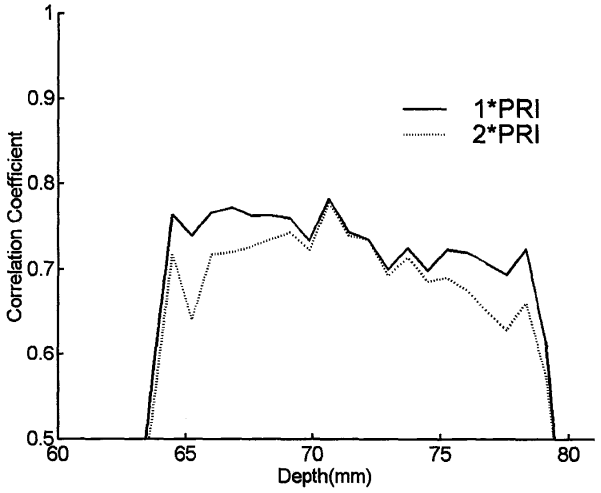

Fig. 11. Correlation coefficient as a function of depth with an SNR of 9.5 dB. Solid is for two signals separated by one PRI, and dotted is for two signals separated by two PRIs.

be compensated. However, it was also shown that significant errors are present when estimating flow gradients and correlation coefficients. Although signal averaging can be used to reduce such errors, averaging is not applicable to pulsatile flows, and it limits clinical utility of the correlation method.

In the presence of flow gradients, speckle decorrelation depends on the correlation size as demonstrated in Fig. 6 and Fig. 9. Ideally, it is desirable to be able to estimate and compensate for effects of flow gradients on decorrelation. In practice, however, such a scheme is difficult to develop because of the following problems. First, the stan-

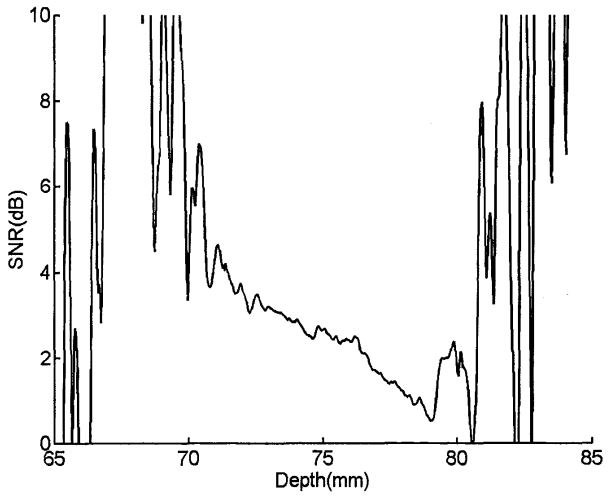

Fig. 12. SNR as a function of depth from the experiment data.

dard deviation of the correlation coefficient estimation is significant. Given a single measurement, the estimated correlation coefficient may be very different from its mean value. The error in correlation coefficient may lead to a significantly larger error in the estimated velocity. Thus, unless signal averaging can be applied, such a method is not feasible. However, application of signal averaging is limited in practice because of the time varying nature of physiological flows.

Speckle decorrelation is also affected by the SNR. Because the SNR is depth dependent, effects of the SNR on speckle decorrelation also change with depth. Note that the SNR plays a more critical role in extracorporeal applications where the SNR is typically low. In this case, the application of speckle decorrelation on flow estimation is more difficult. For other clinical applications with a high SNR (e.g., IVUS), success of the decorrelation method has been reported [3], [4].

As shown in Fig. 9, the correlation coefficient may increase as the kernel size increases because of the improvement in SNR. Such an increase was absent from Fig. 6, where no noise was added. Thus, given a flow gradient and an SNR, an optimal correlation kernel size can be found to minimize estimation errors. Such an optimal size is a trade-off between the two factors, as a shorter kernel is desired to minimize flow gradient effects and a longer kernel is desired to improve SNR. With an optimal correlation kernel size, accuracy of the correlation method can be improved but may still be inadequate for quantitative flow measurements.

ACKNOWLEDGMENT

The authors thank the reviewers for insightful comments.

REFERENCES

[1] L.A.F. Ledoux, J. M. Willigers, P. J. Brands, and A.P.G. Hoeks, "Experimental verification of the correlation behavior of analytic ultrasound radiofrequency signals received from moving structures," *Ultrasound Med. Biol.*, vol. 24, no. 9, pp. 1383–1396, 1998.

[2] ——, "Angle-independent measurement by correlation of ultrasound signals assessed with a single circular-shaped transducer," *Ultrason. Imaging*, vol. 21, no. 3, pp. 216–240, 1999.

[3] W. Li, A.F.W. van der Steen, C. T. Lancee, I. Céspedes, and N. Bom, "Blood flow imaging and volume flow quantitation with intravascular ultrasound," *Ultrasound Med. Biol.*, vol. 24, no. 2, pp. 203–214, 1998.

[4] J. R. Crowe, B. M. Shapo, D. N. Stephens, D. Bleam, M. J. Eberle, E. I. Céspedes, C.-C. Wu, D.W.M. Muller, J. A. Kovatch, R. J. Lederman, and M. O'Donnell, "Blood speed imaging with an intraluminal array," *IEEE Trans. Ultrason., Ferroelect., Freq. Contr.*, vol. 47, no. 3, pp. 672–681, 2000.

[5] B. H. Friemel, L. N. Bohs, K. R. Nightingale, and G. E. Trahey, "Speckle decorrelation due to two-dimensional flow gradients," *IEEE Trans. Ultrason., Ferroelect., Freq. Contr.*, vol. 45, no. 2, pp. 317–326, 1998.

[6] P.-C. Li and M. O'Donnell, "Elevational spatial compounding," *Ultrasound Imaging*, vol. 16, no. 3, pp. 176–189, 1994.

[7] A. T. Kerr and J. W. Hunt, "A method for computer simulation of ultrasound Doppler color flow images—II. Simulation results," *Ultrasound Med. Biol.*, vol. 18, no. 10, pp. 873–879, 1992.

[8] C. Kasai, K. Namekawa, A. Koyano, and R. Omoto, "Real-time two dimensional blood flow imaging using an autocorrelation technique," *IEEE Trans. Sonics Ultrason.*, vol. 32, no. 3, pp. 458–464, 1985.

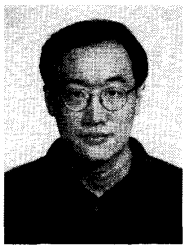

Pai-Chi Li (S'91–M'93–S'93–M'95) received the B.S. degree in electrical engineering from National Taiwan University, Taipei, Taiwan, R.O.C. in 1987 and the M.S. and Ph.D. degrees from the University of Michigan, Ann Arbor in 1990 and 1994, respectively, both in electrical engineering: systems.

He was a research assistant with the Department of Electrical Engineering and Computer Science from 1990 to 1994. He joined Acuson Corporation (Mountain View, CA) as a member of the Technical Staff in June 1994. His work in Acuson was primarily in the areas of medical ultrasonic imaging system design for both cardiology and general imaging applications. In August 1997, he went back to the Department of Electrical Engineering at National Taiwan University as Assistant Professor. He then became Associate Professor in August 1998. His current research interests include biomedical ultrasonic imaging and signal processing.

Dr. Li is a member of IEEE, and he was the recipient of the Distinguished Achievement Award in Electrical Engineering: Systems for his outstanding academic achievement at the University of Michigan.

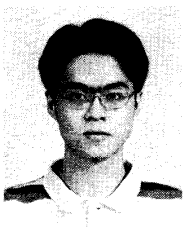

Chong-Jing Cheng was born in Taiwan, R.O.C. on October 6, 1975. He received the B.S. and M.S. degrees in electrical engineering from National Taiwan University in 1998 and 2000, respectively. His current research interest is ultrasound flow velocity estimation.

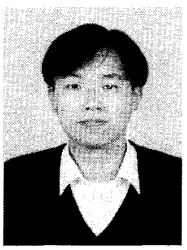

Chih-Kuang Yeh was born in 1973 in Taiwan, R.O.C. He received the B.S. and M.S. degrees in biomedical engineering from Chung-Yuan Christian University and National Cheng-Kung University in 1995 and 1997, respectively. Currently, he is a Ph.D. candidate in the Department of Electrical Engineering, National Taiwan University. His current research interest is ultrasonic flow velocity estimation.